Performance Analysis of Hybrid Underwater Wireless System for Shallow Sea Monitoring.

Romya Bhatnagar
Netaji Subhas University of Technology
Parul Garg (parul_saini@yahoo.co.in)
Netaji Subhas University of Technology

Research Article

Keywords: Optical sensor node, acoustic sensor node, optical acoustic communication node, decode-and-forward relaying, underwater acoustic channel, underwater optical wireless communications

Posted Date: March 6th, 2023

DOI: https://doi.org/10.21203/rs.3.rs-2606335/v1

Additional Declarations: No competing interests reported.

Version of Record: A version of this preprint was published at Photonic Network Communications on September 3rd, 2023. See the published version at https://doi.org/10.1007/s11107-023-01003-2.

Performance Analysis of Hybrid Underwater Wireless System for Shallow Sea Monitoring

Romya Bhatnagar · Parul Garg*

Received: date / Accepted: date

Abstract This paper investigates the performance of hybrid dual hop underwater system which has been proposed for monitoring vast region under shallow sea environment. This hybrid underwater opto-acoustic sensor network (UOASN) is designed to provide higher data rates and less propagation delay with respect to traditional acoustic underwater systems, by including optical carrier. An acoustic sensor and an optical sensor are mounted on shallow water floor at different locations that acquire the surrounding information and transmit it continuously to the underwater vehicle based on round-robin scheduling. Such vehicle is comprised of decode-and-forward relaying mechanism. The underwater acoustic link is determined by α-$\mathcal{F}$ fading distribution and underwater optical link follows the mixture Exponential-Generalized Gamma (EGG) model to characterize channel irradiance fluctuations. The novel closed form expressions for various end to end (E2E) signal to noise ratio (SNR) statistics such as equivalent probability density function (PDF), cumulative distribution function (CDF) and moments have been derived. The analytical expressions are also obtained for outage probability, average bit error rate, ergodic capacity and outage capacity. Besides, the closed form asymptotic expressions for outage probability and average bit error rate are derived.

Keywords Optical sensor node · acoustic sensor node · optical acoustic communication node · decode-and-forward relaying · underwater acoustic channel · underwater optical wireless communications

Romya Bhatnagar
Division of Electronics and Communication Engineering, Netaji Subhas University of Technology, Sector 3, Dwarka, New Delhi, 110078, India
Tel.: +91-9716450225
E-mail: romyabhatnagar.a1@gmail.com

* Corrosponding Author:Parul Garg
Division of Electronics and Communication Engineering, Netaji Subhas University of Technology, Sector 3, Dwarka, New Delhi, 110078, India
E-mail: parul_saini@yahoo.co.in

1 Introduction

Challenges, that are being faced by underwater communication, have given an innovation to the wireless communication across marine conditions in the recent years. Rivers, lakes, seas, oceans etc are associated with various monitoring activities like earthquake warning system, oil leaks surveillance, oil and fuel extraction, pressure and temperature measurement [1] etc. For such activities, various types of underwater wireless carriers can be used like radio-frequency wave, magnetic induction, acoustic wave and optical wave. Distance achieved, attenuation of signal, bandwidth requirement and data rates are the main factor in selecting the mode of communication. Underwater RF communication allows only short link range through water medium, for instance, at 100 Hz the free space wavelength is 3000 km while in sea water it is only 176 m [2, Table 2]. In case of underwater magnetic field (MF) communication, a moderate transmission distance of 10-100 m is achieved but with less data rates (Mbps) [3]. Long-distance communication provided by widely used underwater acoustics is supported at low frequencies, in turn there is limited bandwidth available [4]. The low speed of underwater acoustic wave (1500m/s) lays out the low data rates (Kbps) with high propagation delay. Many favourable characteristics are associated with underwater optical communication like almost negligible

latency, higher data rates (Gbps) and average transmission distance [5], which makes this technology a very promising one.

In relative to the amenities corresponding to the mentioned underwater communication methods, the combination of them can add extra value to the system network which can lead to produce high data rates, wide coverage etc. Various hybrid acoustic and optical networks have been designed and investigated so far. In [6], network modelling and an energy-efficient strategy for underwater opto-acoustic sensor network (UOASN) have been proposed to determine that how to reduce energy consumption. An underwater hybrid network, which is equipped with an intermediate node carrying optical and acoustic modems, have been proposed showing that this hybrid network is better in energy consumption and throughput than the network comprising only acoustic sensors [7]. Authors in [8] have given a mixture acoustic-optical underwater communication solution for figuring out the exact localization and tracking control of the mobile vehicle. A cooperative routing algorithm in [9] and SectOR protocol for underwater hybrid network in [10] are developed dealing in networking tasks. Mainly, the research over Acoustic/Optical hybrid underwater systems have been carried out on network layer and this has become the driving force to explore the physical layer of such underwater hybrid relayed wireless sensor networks.

Relaying technique is an efficient way to increase the communication range of underwater acoustic sensor networks as well as underwater optical networks and also is an efficacious method to minimize the energy consumption [11–14]. Moreover, decode-and-forward relay (DF) has less impact of noise as it deals with the process of decoding and re-encoding of signal at the node. In literature, many terrestrial and underwater mixed wireless networks using DF relay have been investigated and analysed [15–19] to demonstrate their feasibility.

For an underwater acoustic channel (UAC), there is always a situation to give a thought to select a proper propagation model. Hitherto, there is no certain defined model for the statistical characterization of underwater acoustic channels[20]. In [21], shallow water acoustic communication channel is statistical characterized by Rician distribution. Also in [22], under the assumption of rician fading channel, the performance of single carrier cooperative underwater acoustic communication network has been investigated. Authors in [23] have assumed a Rayleigh fading for underwater multipath acoustic propagation. According to references in [24], it is mentioned that fast fading can be modelled by Rayleigh, Rician, Nakagami-m and compound $\mathcal{K}$-distributions according to data gathered from various field experiments and for large-scale shadowing Lognormal distribution can be implied. So here, UAC having small-scale fast fading and large-scale shadowing is chosen to be characterized by Nakagami-Lognormal distribution. Further, author of [25] has proposed a new well-structured composite fading distribution for UAC which considers shadowing effect, multipath fading and non-linearity of the transmission medium altogether. The α-$\mathcal{F}$ distribution provides a perfect match with the empirical data of underwater acoustic communication, compared with $\mathcal{K}$ and α-μ distributions concurs with other distributions (α-μ distribution and Fisher-Snedecor $\mathcal{F}$ distribution) as special or limiting cases. This distribution is considered to be more flexible model, advantageous than Nakagami-m and provides high consistency with its measured data, so it gives better results for underwater acoustic communications [26].

In earlier times, the characteristic distribution (Lognormal) followed by free space optical (FSO) atmospheric turbulence was generally adopted for irradiance fluctuations of optical signal in water medium [27,28]. Later in [29], the modelling of irradiance fluctuations of UWOC channels, due to the presence of air bubbles in both salty and fresh waters, is done by mixture Exponential-Lognormal distribution, but its analysis is difficult due to the numerical intractability. Fluctuations of light intensity in underwater, due to salinity gradient and due to non-turbulent temperature gradient, was characterized by Weibull distribution [30] and Generalized Gamma distribution (GGD) [31], respectively. In [32], a two-lobe statistical model (mixture Exponential- Gamma distribution) was proposed to characterize irradiance fluctuations of underwater optical signal only under the presence of air bubbles under uniform water temperature. But authors in [33], have presented a more realistic statistical model for UWOC channels which considers characterization of turbulence-induced fading depending upon different levels of air bubbles and temperature gradients present in both fresh and salty waters. It is mixture Exponential-Generalized Gamma (EGG) distribution model.

In this paper, a hybrid UOASN is proposed that provides large geographic area coverage in shallow sea water. As we know, traditional underwater acoustic systems provide communication at long distances with low data rates but on the contrary, optical sensors are frequently employed for short-range communication. In case of exclusive underwater optical networks, numerous nodes must be put at various water depths to collect data from the shallow water bed in order to cover a big region. The solution is to create a dual hop hy-

brid Acoustic/Optical underwater monitoring system, in which a nearby in-range area is covered by an optical connection for short-range communication, and acoustic link is used to pull data from a long distance. The suggested dual hop monitoring system consists of an optical sensor node (OSN) and an acoustic sensor node (ASN), which are deployed near the water's edge according to their communication ranges. To the best of our knowledge, such a hybrid UOASN has not been explored yet in terms of physical parameters in the literature so far. The summary of crucial contributions of this paper are mentioned as:

1) The performance of the hybrid UOASN system, using DF relay protocol, is analysed based on composite α-$\mathcal{F}$ fading distribution used for underwater acoustic link while UOWC link is a mixture EGG channel, considered in thermally uniform salty water.

2) The closed form expression of outage probability and its asymptotic analysis has been yielded to have deeper insights of outage performance. The impact of few parameters on outage probability has been published in [34] and rest of the results have been mentioned in this paper.

3) Derivation of novel closed-form expressions of statistics of end to end (E2E) SNR has been obtained. Also, the analytical expressions of average bit error rate (also in high SNR regime), ergodic capacity, outage capacity are the new contributions of the paper.

The remainder of this paper is classified as: Section II describes the system and channel models. The statistical properties of the E2E SNR of the links using DF relay protocol are presented in Section III. Section IV contains, the performance metrics derivations and their analysis along with exact closed-form expressions. Section V lays out analytical output and discussions. Finally, conclusions are given in Section VI.

2 SYSTEM AND CHANNEL MODELS

2.1 System Model

In Fig. 1, an uplink hybrid functional model is presented that consists of two static sensor modems (acoustic and optical) mounted at sea floor serving as data collector nodes as well as source (s) to transmit the measured surrounding parameters. The central part of the model consist of a static optical acoustic communication node (OACN) which acts as relay (r). This OACN is an autonomous underwater vehicle (AUV) and is equipped with both acoustic and optical modems along with decode-and-forward relay protocol. This hybrid dual-hop underwater monitoring system works under round-robin scheduling due to which it has two

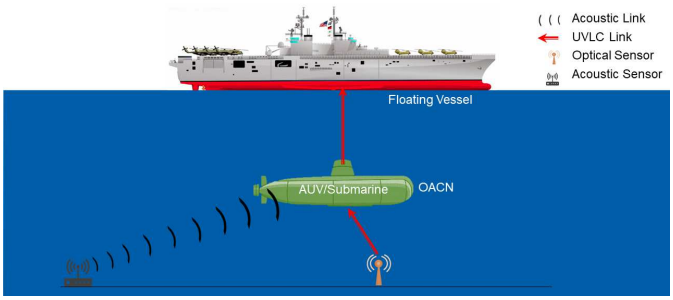

Fig. 1 System Model Elevated View

configurations: 1) Acoustic/Optical wireless monitoring system, 2) Optical/Optical wireless monitoring system. We assume continuous data transmission from both the sensor nodes towards OACN under dynamic TDMA technique is used to support data of different rates. According to different propagation speeds and data rates, the number of time slots for each sensor are reserved and data is scheduled in round-robin manner.This works on assigning the particular fixed time slots in a periodical way. Details of underwater monitoring system are given as below:

1)*Acoustic/Optical wireless monitoring system*: For underwater remote area monitoring, first hop is the acoustic link, which has an acoustic sensor node or source (s) that sends the acquired data to OACN or relay (r). Further, data is transferred on optical carrier to the destination node (d), present on the water surface in the form of floating vehicle or bouy.

2)*Optical/Optical wireless monitoring system*: For monitoring underwater close proximity region, both of the information bearer links of the dual hop relaying system are chosen to be optical. The measured data from surroundings is transmitted to the same destination node through common OACN from the sea floor mounted optical sensor modem.

2.2 Channel Model

In this section, modeling of both acoustic and optical channels of the proposed system are introduced for the analysis of system performance.

2.2.1 Underwater Acoustic Link

For underwater acoustic link, we have assumed α-$\mathcal{F}$ composite fading distribution. The probability density

function (PDF) of the instantaneous SNR γ_A of source to relay acoustic link [25] is given by

$$f_{\gamma_A}(\gamma) = \frac{\alpha_i \chi_i^{m_i}}{2B(\mu_i, m_i)} \gamma^{\frac{\alpha_i \mu_i}{2}} \times (\gamma^{\frac{\alpha_i}{2}} + \chi_i)^{-(\mu_i + m_i)} \quad (1)$$

where B(.,.) is the Beta function, $\chi_i = \frac{(m_i-1)\bar{\gamma}_{sr}^{\frac{\alpha_i}{2}}}{\mu_i \lambda^{\frac{\alpha_i}{2}}}$ and λ is defined as

$$\lambda = (\frac{m_i-1}{\mu_i})^{\frac{2}{\alpha_i}} \frac{\Gamma(\mu_i + \frac{2}{\alpha_i})\Gamma(m_i - \frac{2}{\alpha_i})}{\Gamma(\mu_i)\Gamma(m_i)}, m_i > \frac{2}{\alpha_i}$$

where $\Gamma(x) = (x-1)!$. We determine, α_i as the power parameter that determines the nonlinearity of the propagation media with the condition $\alpha_i > 0$, m_i and μ_i are the shadowing parameter and number of multipath components, respectively. The value of μ_i varies from 1 to 10 (worse multipath to good multipath condition) whereas m_i has different values as 1.1 (heavy shadowing), 5 (moderate shadowing) and 50 (light shadowing)[25]. On applying [35, 8.4.2.5] and then [36, 16.19.2], the PDF can be represented, in terms of Meijer's G function, as

$$f_{\gamma_A}(\gamma) = G_{1,1}^{1,1}\left(\frac{\gamma^{\frac{\alpha_i}{2}}}{\chi_i} \middle| \begin{matrix} 1-m_i \\ \mu_i \end{matrix} \right) \quad (2)$$

where $\eta_o = \frac{1}{\Gamma(\mu_i)\Gamma(m_i)}$ Using $F_\gamma(\gamma) = \int_0^\gamma f_\gamma(x)dx$, [37, 3.194.1] and [38, 2.9.15], the CDF of the instantaneous SNR γ_A can be expressed as

$$F_{\gamma_A}(\gamma) = \eta_o G_{2,2}^{1,2}\left(\frac{\gamma^{\frac{\alpha_i}{2}}}{\chi_i} \middle| \begin{matrix} 1-m_i, 1 \\ \mu_i, 0 \end{matrix} \right) \quad (3)$$

2.2.2 Underwater Optical Link

Here, turbulence induced fading underwater wireless optical link is presumed to be Exponential-Generalized Gamma (EGG) distributed. This model includes air bubble levels and temperature gradient to characterize fading in both fresh and salty waters. The PDF for instantaneous SNR γ_{O_l} [33] is given as

$$f_{\gamma_{O_l}}(\gamma) = \frac{\omega}{r\gamma} G_{0,1}^{1,0}\left(\sigma_l \gamma^{\frac{1}{r}} \middle| \begin{matrix} - \\ 1 \end{matrix} \right) + \frac{C(1-\omega)}{r\gamma\Gamma(A)} G_{0,1}^{1,0}\left(\rho_l \gamma^{\frac{C}{r}} \middle| \begin{matrix} - \\ A \end{matrix} \right) \quad (4)$$

with

$$\sigma_l = \frac{1}{y(\mu_{r_l})^{\frac{1}{r}}}, \rho_l = \frac{1}{B^C(\mu_{r_l})^{\frac{C}{r}}}$$

where link $l = sr$, rd denoting the link between optical sensor node to OACN and OACN to floating vessel link, respectively. μ_{r_l} is the average electrical SNR with values ($r = 1$) and ($r = 2$) for heterodyne detection and IM/DD technique, respectively. The average electrical SNR for heterodyne detection is determined as $\mu_{1_l} = \bar{\gamma}_l$

Table 1 Estimated Parameters of the Optical Link Under Uniform Temperature for Salty Water

BL (L/min)	ω	y	A	B	C
2.4	0.1770	0.4687	0.7736	1.1372	49.1773
4.7	0.2064	0.3953	0.5307	1.2154	35.7368
7.1	0.4344	0.4747	0.3935	1.45061	77.0245
16.5	0.4951	0.1368	0.0161	3.2033	82.1030

and for intensity modulation/direct detection, the average electrical SNR is given as

$$\mu_{2_l} = \frac{\bar{\gamma}_l}{2\omega y^2 + \frac{B^2(1-\omega)\Gamma(A+\frac{2}{C})}{\Gamma(A)}} \quad (5)$$

The parameters A, B and C are related to the Generalized Gamma distribution and y belongs to Exponential distribution. The range of mixture coefficient of both the distributions as ω, varies from 0 to 1. Table I represents the values of parameters of the EGG distribution for thermally uniform UWOC link under salty water conditions with different air bubble levels which are taken from [33]. The CDF of instantaneous SNR γ_{O_l} of underwater optical channel can be framed by integrating (4) and presented as

$$F_{\gamma_{O_l}}(\gamma) = \omega G_{1,2}^{1,1}\left(\sigma_l \gamma^{\frac{1}{r}} \middle| \begin{matrix} 1 \\ 1, 0 \end{matrix} \right) + \frac{(1-\omega)}{\Gamma(A)} G_{1,2}^{1,1}\left(\rho_l \gamma^{\frac{C}{r}} \middle| \begin{matrix} 1 \\ A, 0 \end{matrix} \right) \quad (6)$$

3 Statistical analysis of End to End SNR

This section contains the closed form mathematical expressions for various statistics of the proposed hybrid UOASN system such as equivalent CDF, PDF, generalised moments, etc of end-to-end instantaneous SNR. Under the assumption of DF relay scheme, the corresponding E2E SNR of dual hop system γ_{DH} is given by

$$\gamma_{DH} = min(\gamma_1, \gamma_2) \quad (7)$$

where γ_1 and γ_2 represent the value of instantaneous SNR of underwater first hop and second hop, applicable to either of the two models. Under DF relaying protocol, the equivalent CDF and PDF of the dual hop system [38, Eq.(37)] is given as

$$F_{\gamma_{1/2}}(\gamma) = F_{\gamma_1}(\gamma) + F_{\gamma_2}(\gamma) - F_{\gamma_1}(\gamma)F_{\gamma_2}(\gamma) \quad (8)$$

$$f_{\gamma_{1/2}}(\gamma) = f_{\gamma_1}(\gamma) + f_{\gamma_2}(\gamma) - F_{\gamma_1}(\gamma)f_{\gamma_2}(\gamma) - f_{\gamma_1}(\gamma)F_{\gamma_2}(\gamma) \quad (9)$$

3.1 Acoustic/Optical Wireless Monitoring System

3.1.1 Cumulative Distribution Function

Using (3), (6) and (8), the equivalent CDF of SNR $\gamma_{A/O}$ of Acoustic/Optical dual hop system having relay to destination optical link can be given as (10).

For yielding asymptotic analysis, the general condition is carried at $\bar{\gamma} \to \infty$. The expression of CDF in high SNR regime $F^{\infty}_{\gamma_{A/O}}(\gamma)$ can be obtained by substituting asymptotic expressions of CDF of instantaneous SNR of acoustic link as well as optical link in (8) which are derived, using [38, Eq.(2.9.1)] and [38, Eq.(1.8.4)], as

$$F^{\infty}_{\gamma_A}(\gamma) = \frac{\eta_o \Gamma(\mu_i + m_i)}{\mu_i} \left(\frac{\mu_i \lambda^{\frac{\alpha_i}{2}} \gamma^{\frac{\alpha_i}{2}}}{(m_i - 1)\bar{\gamma}_{sr}^{\frac{\alpha_i}{2}}} \right)^{\mu_i} \tag{11}$$

$$F^{\infty}_{\gamma_{O_{rd}}}(\gamma) = \frac{\omega}{y} \left(\frac{\gamma}{\mu_{r_{rd}}} \right)^{\frac{1}{r}} + \frac{(1-\omega)}{\Gamma(A+1)} \left(\frac{\gamma}{B^r \mu_{r_{rd}}} \right)^{\frac{AC}{r}} \tag{12}$$

3.1.2 Probability Density Function

On substituting (2), (3), (4) and (6) in (9) , the equivalent PDF is represented as in (13) with values $\varrho = \frac{\alpha_i}{2\Gamma(\mu_i)\Gamma(m_i)}, \eta_1 = \frac{\omega}{r}, \eta_2 = \frac{C(1-\omega)}{r\Gamma(A)}$

3.1.3 Generalized Moments

Various statistical parameters like mean, variance etc can be derived using n-th moment of the end-to-end instantaneous SNR γ. According to the definition, the n-th moment can be derived through

$$E\langle \gamma^n \rangle = \int_0^{\infty} \gamma^n f_{\gamma}(\gamma) d\gamma \tag{14}$$

Now, substituting (13) in (14) results in generalized expression of n-th moment in terms of gamma function as well as univariate Fox's H function [38] as given by (15).

3.2 Optical/Optical Wireless Monitoring System

3.2.1 Cumulative Distribution Function

For this dual hop system, the equivalent CDF $F_{\gamma_{O/O}}(\gamma)$ is yielded by substituting (6) in (8) having $F_{\gamma_{O_{sr}}}(\gamma)$ and $F_{\gamma_{O\,rd}}(\gamma)$ are CDFs of optical sr link and rd link, respectively. The final CDF expression is mentioned as in (16).

The asymptotic CDF expression of all optical dual hop system can be given as $F^{\infty}_{\gamma_{O/O}}(\gamma)$ and it is derived using (8) and $F^{\infty}_{\gamma_{O_l}}(\gamma)$ where

$$F^{\infty}_{\gamma_{O_l}}(\gamma) = \frac{\omega}{y} \left(\frac{\gamma}{\mu_{r_l}} \right)^{\frac{1}{r}} + \frac{(1-\omega)}{\Gamma(A+1)} \left(\frac{\gamma}{B^r \mu_{r_l}} \right)^{\frac{AC}{r}} \tag{17}$$

3.2.2 Probability Density Function

With similar method mentioned for Acoustic/Optical monitoring system , we obtain the expression of equivalent PDF of instantaneous SNR on putting (4) and (6) in (9) which is represented as (18).

3.2.3 Generalized Moments

Using the basic definition as given in (14) , the n-th moment of dual hop Optical/Optical system is presented by (19).

4 Comprehensive Performance Analysis of The Entire Functional Model

4.1 Outage Probability

4.1.1 Exact Analysis

One of the critical performance metrics of the wireless communication system is outage probability. It is regarded as a state of an outage when the instantaneous SNR of the entire communication system falls below the necessary threshold (thres) to be maintained. For the proposed either of the dual hop model, the expression for outage probability is derived as

$$P_{out} = Pr[min(\gamma_1, \gamma_2) < \gamma_{thres}] \tag{20}$$

Assuming all the links to be independent and using (3), (6) and (20) , we can obtain the closed form expressions of outage probability of Acoustic/Optical monitoring system and Optical/Optical monitoring system, respectively.

4.1.2 High SNR Analysis

The observations regarding impact of several dual hop system parameters, on the outage performance of the communication network, are judged by asymptotic analysis. On substituting (11) and (12) in (20) and after some rearrangement the expression of outage probability of Acoustic/Optical system model at high SNR regime is given as

$$P^{\infty}_{out_{A/O}}(\gamma) = \gamma_{th}^{\frac{1}{r}} \Big[\beta_1 + \beta_2 \gamma_{th}{}^{AC} + \beta_3^{\frac{\alpha_i \mu_i r}{2}} \times (1 - \beta_1 \gamma_{th} - \beta_2 \gamma_{th}^{AC}) \Big] \tag{21}$$

where

$\beta_1 = \frac{\omega}{y(\mu_{r_{rd}})^{\frac{1}{r}}}$, $\beta_2 = \frac{(1-\omega)}{\Gamma(A+1)} \frac{\mu_{r_{rd}}^{\frac{-AC}{r}}}{B^{AC}}$,

$\beta_3 = \frac{\mu_i^{\mu_i - 1}}{B(\mu_i, m_i)} \left(\frac{\lambda^{\frac{\alpha_i}{2}}}{m_i - 1} \right)^{\mu} \bar{\gamma}_A^{\frac{-\alpha_i \mu_i}{2}}$

$$F_{\gamma_{A/O}}(\gamma) = 1 - \left[\left(1 - \eta_o G_{2,2}^{1,2}\left(\frac{\gamma^{\frac{\alpha_i}{2}}}{\chi_i}\left|\begin{matrix}1-m_i,1\\ \mu_i,0\end{matrix}\right.\right)\left(1 - \omega G_{1,2}^{1,1}\left(\sigma_{rd}\gamma^{\frac{1}{r}}\left|\begin{matrix}1\\ 1,0\end{matrix}\right.\right) - \frac{(1-\omega)}{\Gamma(A)} G_{1,2}^{1,1}\left(\rho_{rd}\gamma^{\frac{C}{r}}\left|\begin{matrix}1\\ A,0\end{matrix}\right.\right)\right)\right] \tag{10}$$

$$\mathrm{f}_{\gamma_{A/O}}(\gamma) = \frac{1}{\gamma}\left[\left(1 - \frac{2\delta}{\alpha_i} G_{2,2}^{1,2}\left(\frac{\gamma^{\frac{\alpha_i}{2}}}{\chi_i}\left|\begin{matrix}1-m_i,1\\ \mu_i,0\end{matrix}\right.\right)\right)\left(\eta_1 G_{0,1}^{1,0}\left(\sigma_{rd}\gamma^{\frac{1}{r}}\left|\begin{matrix}-\\ 1\end{matrix}\right.\right) + \eta_2 G_{0,1}^{1,0}\left(\rho_{rd}\gamma^{\frac{C}{r}}\left|\begin{matrix}-\\ A\end{matrix}\right.\right)\right)$$
$$+\delta G_{1,1}^{1,1}\left(\frac{\gamma^{\frac{\alpha_i}{2}}}{\chi_i}\left|\begin{matrix}1-m_i\\ \mu_i\end{matrix}\right.\right)\left(1 - r\eta_1 G_{1,2}^{1,1}\left(\sigma_{rd}\gamma^{\frac{1}{r}}\left|\begin{matrix}1\\ 1,0\end{matrix}\right.\right) - \frac{r}{C}\eta_2 G_{1,2}^{1,1}\left(\rho_{rd}\gamma^{\frac{C}{r}}\left|\begin{matrix}1\\ A,0\end{matrix}\right.\right)\right)\Bigg] \tag{13}$$

$$\mathrm{E}\langle\gamma^n\rangle_{A/O} = \omega(y^r\mu_{r_{rd}})^n\Gamma(rn+1) + \frac{(1-\omega)(B^r\mu_{r_{rd}})^n\Gamma(\frac{rn}{C}+A)}{\Gamma(A)} + \eta_0\chi_i^{\frac{2n}{\alpha_i}}\Bigg[\Gamma(\mu_i + \tfrac{2n}{\alpha_i})\Gamma(m_i - \tfrac{2n}{\alpha_i}) - \omega$$
$$\times H_{2,3}^{2,2}\left(\frac{\chi_i^{\frac{2}{r\alpha_i}}}{y\mu_{r_{rd}}^{\frac{1}{r}}}\left|\begin{matrix}(1,1)(1-\mu_i-\frac{2n}{\alpha_i},\frac{2}{r\alpha_i})\\ (1,1)(m_i-\frac{2n}{\alpha_i},\frac{2}{r\alpha_i})(0,1)\end{matrix}\right.\right) - \frac{(1-\omega)}{\Gamma(A)}H_{2,3}^{2,2}\left(\frac{\chi_i^{\frac{2C}{r\alpha_i}}}{B^C\mu_{r_{rd}}^{\frac{C}{r}}}\left|\begin{matrix}(1,1)(1-\mu_i-\frac{2n}{\alpha_i},\frac{2C}{r\alpha_i})\\ (A,1)(m_i-\frac{2n}{\alpha_i},\frac{2C}{r\alpha_i})(0,1)\end{matrix}\right.\right) - \frac{2}{\alpha_i}\eta_1$$
$$\times H_{2,3}^{3,1}\left(\frac{\chi_i^{\frac{2}{r\alpha_i}}}{y\mu_{r_{rd}}^{\frac{1}{r}}}\left|\begin{matrix}(1-\mu_i-\frac{2n}{\alpha_i},\frac{2}{r\alpha_i})(1-\frac{2n}{\alpha_i},\frac{2}{r\alpha_i})\\ (1,1)(m_i-\frac{2n}{\alpha_i},\frac{2}{r\alpha_i})(-\frac{2n}{r\alpha_i},\frac{2}{r\alpha_i})\end{matrix}\right.\right) - \frac{2}{\alpha_i}\eta_2 H_{2,3}^{3,1}\left(\frac{\chi_i^{\frac{2C}{r\alpha_i}}}{B^C\mu_{r_{rd}}^{\frac{C}{r}}}\left|\begin{matrix}(1-\mu_i-\frac{2n}{\alpha_i},\frac{2C}{r\alpha_i})(1-\frac{-2n}{\alpha_i},\frac{2C}{r\alpha_i})\\ (A,1)(m_i-\frac{2n}{\alpha_i},\frac{2C}{r\alpha_i})(\frac{-2n}{\alpha_i},\frac{2C}{r\alpha_i})\end{matrix}\right.\right)\Bigg] \tag{15}$$

Similarly, the asymptotic expression of outage probability for Optical/Optical model can be presented as

$$\mathrm{P}_{out_{O/O}}^{\infty}(\gamma) = \gamma_{th}^{\frac{1}{r}}\Big[2 - (1 - \tfrac{\epsilon_1\xi_1}{\gamma_{th}})(1 + \epsilon_2\xi_2^{AC}) - (1 - \tfrac{\epsilon_1\xi_2}{\gamma_{th}})$$
$$\times(1 + \epsilon_2\xi_1^{AC}) - \epsilon_1^2\xi_1\xi_2 - \epsilon_2^2(\xi_1\xi_2)^{AC}\Big] \tag{22}$$

where

$\epsilon_1 = \frac{\omega}{y}, \epsilon_2 = \frac{(1-\omega)}{B\Gamma(A+1)}, \xi_1 = \gamma_{th}(\frac{1}{\mu_{r_{sr}}})^{\frac{1}{r}},$

$\xi_2 = \gamma_{th}(\frac{1}{\mu_{r_{rd}}})^{\frac{1}{r}}$

4.2 Average Bit Error Rate

4.2.1 Exact Analysis

The performance of the proposed dual hop underwater monitoring models can be determined through an another important metric which is average bit error rate. In case of DF relay protocol, at relay node the signal is decoded and re-encoded before transmitting to the destination node. In such a situation, decoding errors can prevail at any node except sending node and after taking in account such errors, the equivalent average BER for either of dual hop underwater monitoring model can be calculated using

$$P_{e_{1/2}} = P_{e_1}(1 - P_{e_2}) + P_{e_2}(1 - P_{e_1}) \tag{23}$$

where P_{e_1} and P_{e_2} are the respective ABERs of first hop and second hop which depends on the type of modulation used for each link. Now, we will find the ABER for each individual link used in functional model as:

ABER for Acoustic link: For variety of binary digital modulation schemes, the expression of ABER for underwater acoustic link can be given as [40]

$$P_{e_A} = \frac{\varsigma^{\nu}}{2\Gamma(\nu)}\int_0^{\infty} e^{-\varsigma\gamma}\gamma^{\nu-1}F_{\gamma_A}(\gamma)d\gamma \tag{24}$$

having values of (ς, ν) according to Table II. After putting $e^{-\varsigma\gamma}$ from [41, Eq. (01.03.26.0004.01)] in terms of Meijer's G Function as $G_{0,1}^{1,0}\left(\varsigma\gamma\left|\begin{matrix}-\\ 0\end{matrix}\right.\right)$ and (3) in (24) and utilizing [38, Eq. 2.9.1] and [35, Eq. (2.24.2/1)], the ABER for acoustic link is yielded as

$$P_{e_A} = H_{3,2}^{1,3}\left(\frac{\chi_i}{\varsigma^{\frac{\alpha_i}{2}}}\left|\begin{matrix}(1-m_i,1)(1,1)(1-\nu,\frac{\alpha_i}{2})\\ (\mu_i,1)(0,1)\end{matrix}\right.\right)$$
$$\times\frac{\eta_0\varsigma^{-\nu}}{2\sqrt{\pi}} \tag{25}$$

In our system model, we have considered BPSK scheme as modulation type for acoustic link with $(\varsigma, \nu) = (1, 0.5)$.

ABER for Optical link: Under heterodyne ($r = 1$) and IM/DD ($r = 2$) detection techniques, average BER expression for optical link in terms of PDF of instantaneous SNR for different modulation schemes can be expressed as [42]

$$P_{e_{O_l}} = \frac{\varrho}{2\Gamma(p)}\sum_{k=1}^{n}\int_0^{\infty}\Gamma(p, q_k\gamma)f_{\gamma_{O_l}}(\gamma)d\gamma \tag{26}$$

Table 2 Parameters Of Binary Modulation Schemes

Modulation Schemes	ς	ν
Binary Phase Shift Keying	1	0.5
Differential Binary Phase Shift Keying	1	1
Binary Frequency Shift Keying	0.5	0.5

$$\mathrm{F}_{\gamma_{O/O}}(\gamma) = 1 - \left[\left(1 - \omega G_{1,2}^{1,1}\left(\sigma_{sr}\gamma^{\frac{1}{r}} \middle| \begin{matrix} 1 \\ 1,0 \end{matrix} \right) - \frac{(1-\omega)}{\Gamma(A)} G_{1,2}^{1,1}\left(\rho_{sr}\gamma^{\frac{C}{r}} \middle| \begin{matrix} 1 \\ A,0 \end{matrix} \right) \right) \right.$$
$$\left. \times \left(1 - \omega G_{1,2}^{1,1}\left(\sigma_{rd}\gamma^{\frac{1}{r}} \middle| \begin{matrix} 1 \\ 1,0 \end{matrix} \right) - \frac{(1-\omega)}{\Gamma(A)} G_{1,2}^{1,1}\left(\rho_{rd}\gamma^{\frac{C}{r}} \middle| \begin{matrix} 1 \\ A,0 \end{matrix} \right) \right) \right] \tag{16}$$

$$f_{\gamma_{O/O}}(\gamma) = \frac{1}{\gamma} \left[\left(1 - r\eta_1 G_{1,2}^{1,1}\left(\sigma_{rd}\gamma^{\frac{1}{r}} \middle| \begin{matrix} 1 \\ 1,0 \end{matrix} \right) - \frac{r}{C}\eta_2 G_{1,2}^{1,1}\left(\rho_{rd}\gamma^{\frac{C}{r}} \middle| \begin{matrix} 1 \\ A,0 \end{matrix} \right) \right) \left(\eta_1 G_{0,1}^{1,0}\left(\sigma_{sr}\gamma^{\frac{1}{r}} \middle| \begin{matrix} - \\ 1 \end{matrix} \right) \right.\right.$$
$$\left. + \eta_2 G_{0,1}^{1,0}\left(\sigma_{sr}\gamma^{\frac{C}{r}} \middle| \begin{matrix} - \\ A \end{matrix} \right) \right) + \left(1 - r\eta_1 G_{1,2}^{1,1}\left(\sigma_{sr}\gamma^{\frac{1}{r}} \middle| \begin{matrix} 1 \\ 1,0 \end{matrix} \right) - \frac{r}{C}\eta_2 G_{1,2}^{1,1}\left(\rho_{sr}\gamma^{\frac{C}{r}} \middle| \begin{matrix} 1 \\ A,0 \end{matrix} \right) \right)$$
$$\left. \times \left(\eta_1 G_{0,1}^{1,0}\left(\sigma_{rd}\gamma^{\frac{1}{r}} \middle| \begin{matrix} - \\ 1 \end{matrix} \right) + \eta_2 G_{0,1}^{1,0}\left(\sigma_{rd}\gamma^{\frac{C}{r}} \middle| \begin{matrix} - \\ A \end{matrix} \right) \right) \right] \tag{18}$$

$$\mathrm{E}\langle\gamma^n\rangle_{O/O} = \left(\omega y^{rn}\Gamma(rn+1) + \frac{(1-\omega)B^{rn}\Gamma(\frac{rn}{C}+A)}{\Gamma(A)} \right) \left[(\mu_{r_{sr}})^n + (\mu_{r_{rd}})^n \right] - \eta_1 r^2 (y^r \mu_{r_{sr}})^n$$
$$\times \left[\eta_1 H_{2,2}^{2,1}\left(\left(\frac{\mu_{r_{sr}}}{\mu_{r_{rd}}}\right)^{\frac{1}{r}} \middle| \begin{matrix} (-rn,1)(1-rn,1) \\ (1,1)(-rn,1) \end{matrix} \right) + \eta_2 H_{2,2}^{2,1}\left(\left(\frac{y}{B}\right)^C \left(\frac{\mu_{r_{sr}}}{\mu_{r_{rd}}}\right)^{\frac{C}{r}} \middle| \begin{matrix} (-rn,C)(1-rn,C) \\ (A,1)(-rn,C) \end{matrix} \right) \right]$$
$$\text{-}\eta_2 \frac{r^2}{C^2}(B^r \mu_{r_{sr}})^n \left[\eta_1 \Gamma(A) H_{2,2}^{2,1}\left(\left(\frac{B}{y}\right) \left(\frac{\mu_{r_{sr}}}{\mu_{r_{rd}}}\right)^{\frac{1}{r}} \middle| \begin{matrix} (1-A-\frac{rn}{C},\frac{1}{C})(1-\frac{rn}{C},\frac{1}{C}) \\ (1,1)(\frac{-rn}{C},\frac{1}{C}) \end{matrix} \right) \right.$$
$$\left. + \eta_2 H_{2,2}^{2,1}\left(\left(\frac{\mu_{r_{sr}}}{\mu_{r_{rd}}}\right)^{\frac{C}{r}} \middle| \begin{matrix} (1-A-\frac{rn}{C},1)(1-\frac{rn}{C},1) \\ (A,1)(\frac{-rn}{C},1) \end{matrix} \right) \right] - \eta_1 r^2 (y^r \mu_{r_{rd}})^n \left[\eta_1 H_{2,2}^{2,1}\left(\left(\frac{\mu_{r_{rd}}}{\mu_{r_{sr}}}\right)^{\frac{1}{r}} \middle| \begin{matrix} (-rn,1)(1-rn,1) \\ (1,1)(-rn,1) \end{matrix} \right) \right.$$
$$\left. + \eta_2 H_{2,2}^{2,1}\left(\left(\frac{y}{B}\right)^C \left(\frac{\mu_{r_{rd}}}{\mu_{r_{sr}}}\right)^{\frac{C}{r}} \middle| \begin{matrix} (-rn,C)(1-rn,C) \\ (A,1)(-rn,C) \end{matrix} \right) \right]$$
$$\text{-}\eta_2 \frac{r^2}{C^2}(B^r \mu_{r_{rd}})^n \left[\eta_1 \Gamma(A) H_{2,2}^{2,1}\left(\left(\frac{B}{y}\right) \left(\frac{\mu_{r_{rd}}}{\mu_{r_{sr}}}\right)^{\frac{1}{r}} \middle| \begin{matrix} (1-A-\frac{rn}{C},\frac{1}{C})(1-\frac{rn}{C},\frac{1}{C}) \\ (1,1)(\frac{-rn}{C},\frac{1}{C}) \end{matrix} \right) \right.$$
$$\left. + \eta_2 H_{2,2}^{2,1}\left(\left(\frac{\mu_{r_{rd}}}{\mu_{r_{sr}}}\right)^{\frac{C}{r}} \middle| \begin{matrix} (1-A-\frac{rn}{C},1)(1-\frac{rn}{C},1) \\ (A,1)(\frac{-rn}{C},1) \end{matrix} \right) \right] \tag{19}$$

where $\Gamma(.,.)$ is the upper incomplete Gamma function [37, Eq. (8.350.11)], n, ϱ, p and q_k are the parameters mentioned according to [33, Table III]. Now, we evaluate the optical link under on-off keying (OOK) modulation along with IM/DD technique having parameters as (n,ϱ,p,q_k) = (1,1,0.5,0.25). After substituting the expressions of $\Gamma(.,.)$ in terms of Meijer's G function, PDF from (4) and applying [38, Eq. 2.9.1] and [35, Eq. (2.24.2/1)], ABER expression for optical links associated with both underwater montoring system is given as

$$P_{e_{O_l}} = \frac{\omega}{\sqrt{\pi}} H_{2,2}^{1,2}\left(\frac{1}{y}\left(\frac{2}{\sqrt{\mu_{2_l}}}\right) \middle| \begin{matrix} (1,1)(\frac{1}{2},\frac{1}{2}) \\ (1,1)(0,1) \end{matrix} \right)$$
$$+ \frac{(1-\omega)}{\sqrt{\pi}\Gamma(A)} H_{2,2}^{1,2}\left(\frac{1}{B^C}\left(\frac{2}{\sqrt{\mu_{2_l}}}\right)^C \middle| \begin{matrix} (1,1)(\frac{1}{2},\frac{C}{2}) \\ (A,1)(0,1) \end{matrix} \right) \tag{27}$$

The overall expression of ABER for Acoustic/Optical monitoring system is derived using (23), (25) and (27) which is mentioned as in (28). The equivalent ABER expressions for Optical/Optical monitoring system can be yielded using (23) and (25) which is represented by (29).

4.2.2 High SNR Analysis

To obtain average BER in high SNR regime, the expression follows as

$$P_{e_{1/2}}^{\infty} \rightarrow P_{e_1}^{\infty} + P_{e_2}^{\infty} \tag{30}$$

where $P_{e_1}^{\infty}$ and $P_{e_2}^{\infty}$ are the respective asymptotic BER of P_{e_1} and P_{e_2}. The expression for asymptotic BER of acoustic link is derived by substituting (11) in (24) and utilizing [37, Eq.(3.35.3)]it is obtained as

$$P_{e_A}^{\infty} = \frac{\mu_i^{(\mu_i-1)}\lambda^{\frac{\alpha_i\mu_i}{2}}}{2\sqrt{\pi}B(\mu_i,m_i)(m_i-1)^{\mu_i}} \times \frac{(\frac{\alpha_i\mu_i-1}{2})!}{\bar{\gamma}_{sr}^{\frac{\alpha_i}{2}}} \tag{31}$$

Through same procedure, asymptotic BER of optical link can be represented as

$$\mathrm{P}_{e_{A/O}} = \frac{1}{2}\Bigg[1 + \Bigg(\frac{\omega}{\sqrt{\pi}} H^{1,2}_{2,2}\left(\frac{1}{y}\left(\frac{2}{\sqrt{\mu_{2_{rd}}}}\right) \Bigg| \begin{matrix}(1,1)(\frac{1}{2},\frac{1}{2})\\(1,1)(0,1)\end{matrix}\right) + \frac{(1-\omega)}{\sqrt{\pi}\Gamma(A)} H^{1,2}_{2,2}\left(\frac{1}{B^C}\left(\frac{2}{\sqrt{\mu_{2_{rd}}}}\right)^C \Bigg| \begin{matrix}(1,1)(\frac{1}{2},\frac{C}{2})\\(A,1)(0,1)\end{matrix}\right) - 1\Bigg)$$
$$\times\left(1 - \frac{\eta_0 \varsigma^{-\nu}}{\sqrt{\pi}} H^{1,3}_{3,2}\left(\frac{M}{\varsigma^{\frac{\alpha_i}{2}}} \Bigg| \begin{matrix}(1-m_i,1)(1,1)(1-\nu,\frac{\alpha_i}{2})\\(\mu_i,1)(0,1)\end{matrix}\right)\right)\Bigg] \tag{28}$$

$$\mathrm{P}_{e_{O/O}} = \frac{1}{2}\Bigg[1 - \Bigg\{1 - 2\Bigg(\frac{\omega}{\sqrt{\pi}} H^{1,2}_{2,2}\left(\frac{1}{y}\left(\frac{2}{\sqrt{\mu_{2_{sr}}}}\right) \Bigg| \begin{matrix}(1,1)(\frac{1}{2},\frac{1}{2})\\(1,1)(0,1)\end{matrix}\right) + \frac{(1-\omega)}{\sqrt{\pi}\Gamma(A)} H^{1,2}_{2,2}\left(\frac{1}{B^C}\left(\frac{2}{\sqrt{\mu_{2_{sr}}}}\right)^C \Bigg| \begin{matrix}(1,1)(\frac{1}{2},\frac{C}{2})\\(A,1)(0,1)\end{matrix}\right)\Bigg)\Bigg\}$$
$$\times\Bigg\{1 - 2\Bigg(\frac{\omega}{\sqrt{\pi}} H^{1,2}_{2,2}\left(\frac{1}{y}\left(\frac{2}{\sqrt{\mu_{2_{rd}}}}\right) \Bigg| \begin{matrix}(1,1)(\frac{1}{2},\frac{1}{2})\\(1,1)(0,1)\end{matrix}\right) + \frac{(1-\omega)}{\sqrt{\pi}\Gamma(A)} H^{1,2}_{2,2}\left(\frac{1}{B^C}\left(\frac{2}{\sqrt{\mu_{2_{rd}}}}\right)^C \Bigg| \begin{matrix}(1,1)(\frac{1}{2},\frac{C}{2})\\(A,1)(0,1)\end{matrix}\right)\Bigg)\Bigg\}\Bigg] \tag{29}$$

$$P^{\infty}_{e_{O_l}} = \frac{1}{2\sqrt{\pi}}\Bigg[\frac{2\omega}{y\sqrt{\mu_{2_l}}} + \frac{(1-\omega)}{\Gamma(A+1)}\left(\frac{2}{B\sqrt{\mu_{2_l}}}\right)^{AC}$$
$$\times\Gamma\left(\frac{AC+1}{2}\right)\Bigg] \tag{32}$$

Upon utilizing (30), (31) and (34), we can obtain the closed form expressions for either of the underwater monitoring systems.

4.3 Ergodic capacity

According to definition, the ergodic capacity can be formulated as

$$\mathcal{C}_{erg} = \int_0^{\infty} \log_2(1+\gamma) f_\gamma(\gamma) d\gamma \tag{33}$$

under the heterodyne detection technique, which is approximated based on the analysis given in [43, Eq. (16)] as

$$\mathcal{C}_{erg} \approx \log_2(e)\left[\ln(1+\psi_1) - \frac{\psi_2 - \psi_1^2}{2(1+\psi_1)^2}\right] \tag{34}$$

where ψ_1 and ψ_2 are the first order and second order moments, respectively. For heterodyne detection technique, the expressions of generalized moments are substituted in (34) from (15) in case of Acoustic/Optical monitoring system and for Optical/Optical monitoring system (19) is substituted in (34), to yield the ergodic capacity in each case, respectively. For obtaining the expressions we use order values as $n = 1$ and $n = 2$ along with $r = 1$.

4.4 Outage capacity

The end-to-end outage capacity is determined as the likelihood that the total throughput of the dual hop link falls below a certain value of outage rate C_{Th}. The average throughput outage of the given system is described by this metric. Numerically, this rate can be obtained as in [44] as follows

$$\mathcal{R}(C_{Th}) = Pr[\overline{C} < C_{Th}] = F_\gamma\left(\frac{2^{C_{Th}-1}}{\tau}\right) \tag{35}$$

where $\tau = 1$ for heterodyne detection and $\tau = \frac{e}{2\pi}$ for IM/DD technique. After replacing γ in (10) and (16) according to (35), the expression of outage capacity can be obtained for both the systems.

5 Analytical Results And Discussions

In this section, we present the numerical outcomes for the yielded performance metrics to analyze the effect of numerous parameters associated with underwater acoustic link as well as underwater optical link. Here, all results are carried out for uniform temperature of salty water.

In Fig. 2, the impact of non-linearity of transmission medium α_i along with SNR threshold is exhibited on the outage performance of Acoustic/Optical underwater system in the presence of salty water with bubble level as 2.4 BL/min under heterodyne detection. The low value of $\alpha_i = 1.85$ makes the system to attain a constant value of outage probability from rd link avg. SNR value of 30 dB. Whereas, no such implications are depicted for α_i= 3.75. Higher value of non-linearity factor of medium makes the system favourable. The asymptotic behaviour expressed by (21) follows the inclination of the outage curves in high SNR regime.

The dual hop Optical/Optical system has been analysed under weak case of turbulence with heterodyne detection technique in Fig.3. The curves have been plotted for different SNR threshold values at 40 dB sr link average SNR. Values below 40 dB, drives the system to have negligible impact of rd link average SNR on system's outage performance. As depicted, at higher values of threshold SNR threshold, the system underperforms.

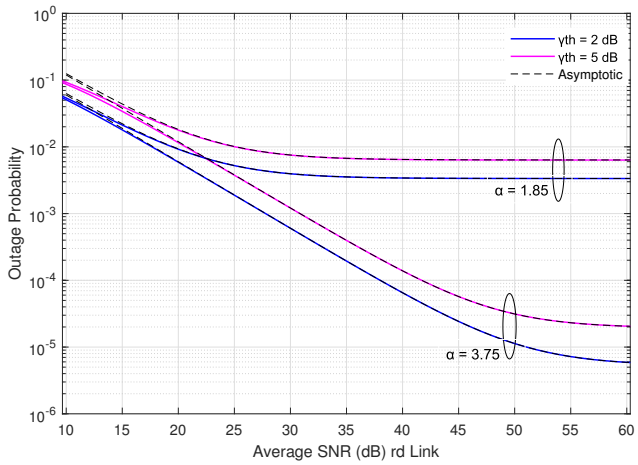

Fig. 2 Outage Probability curves of dual-hop Acoustic/Optical DF relaying system for different values of α_i and threshold SNR under thermally uniform salty water having bubble level as 2.4 BL/min with heterodyne technique having $\mu_i = 1$, $m_i = 5$.

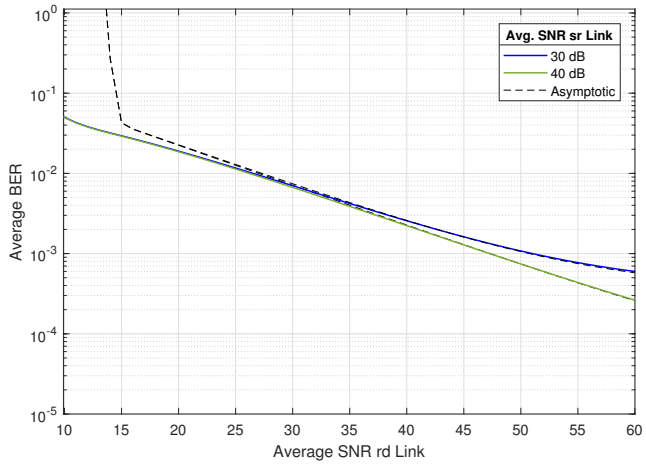

Fig. 4 Average BER of dual hop Acoustic/Optical DF relaying system comparing the performance under moderate shadowing ($m_i = 5$) for different values of sr link avg. SNR having thermally uniform salty water with bubble level as 2.4 BL/min is yielded under IM/DD technique.

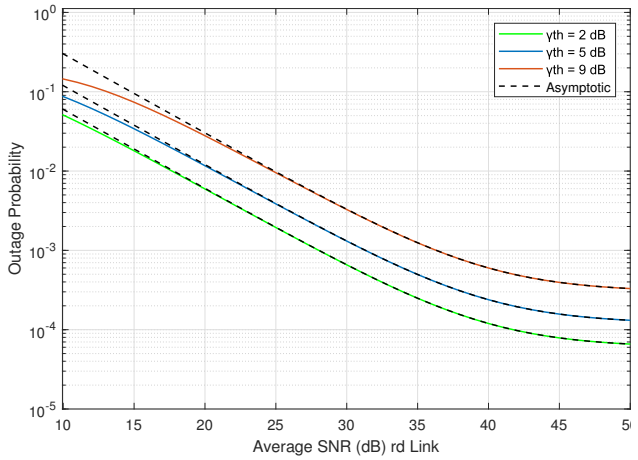

Fig. 3 Outage Probability vs. Average SNR for different values of threshold SNR for Optical/Optical system using DF relaying having thermally uniform water with weak turbulence (2.4 BL/min and salty water) under heterodyne technique.

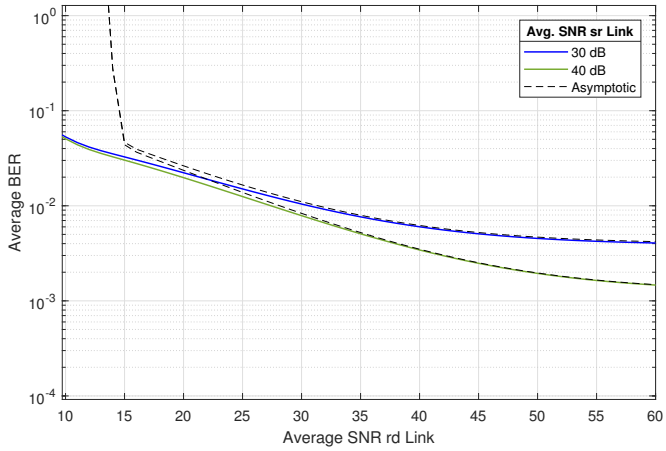

Fig. 5 Effect of variation of Average SNR of sr link on Average BER of Optical/Optical DF relaying system under thermally uniform salty water having bubble level as 2.4 BL/min and IM/DD detection technique.

For both the models, the effect of variation of average SNR of first hop on the total average BER of dual hop systems are demonstrated in Fig. 4 and 5 for Acoustic/Optical and Optical/Optical monitoring systems, respectively. For Acoustic/Optical case in Fig. 4, the basic underwater acoustic scenario is moderate shadowing mode having $m_i = 5$ along with $\alpha_i = 1.85$, $\mu_i = 1$ and optical link is analysed for weak turbulence case. The curves are plotted to compare the profoundness of varying average SNR of sr link. Similarly, in Fig.5, curves of BER (avg sr SNR= 30 dB and 40 dB) of Optical/Optical case are plotted to show the impact of sr link average SNR. The change of 10 dB in acoustic link average SNR has reduced affect on the system's error rate rather than the equivalent difference in average SNR of optical sr link creates distinguished impact as shown in Fig.5. On decreasing the average SNR of source to relay link, average BER of whole system depreciates considerably. The insight of asymptotic behaviour are also represented through plots in each case.

In Fig. 6, we plot the ergodic capacity (in bits per second per hertz) of dual hop Acoustic/Optical for three categories of underwater optical turbulence from weak to severe under heterodyne detection technique ($r = 1$). For the given conditions of acoustic link having moderate shadowing and poor multipath ($\alpha_i = 1.85$, $\mu_i = 1$,

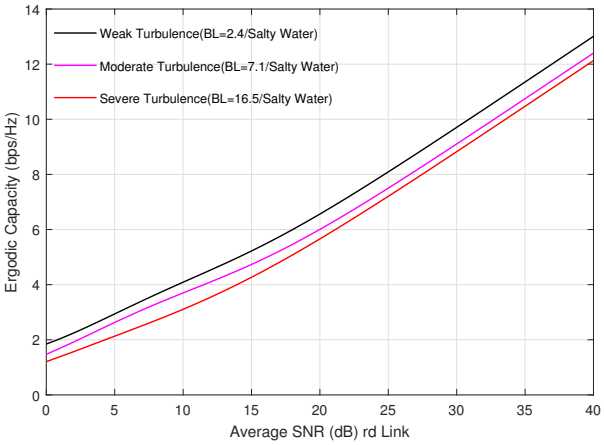

Fig. 6 Ergodic Capacity versus Average SNR showing the impact of underwater weak to severe optical turbulence conditions on a dual-hop Acoustic/Optical system for DF relaying under heterodyne technique.

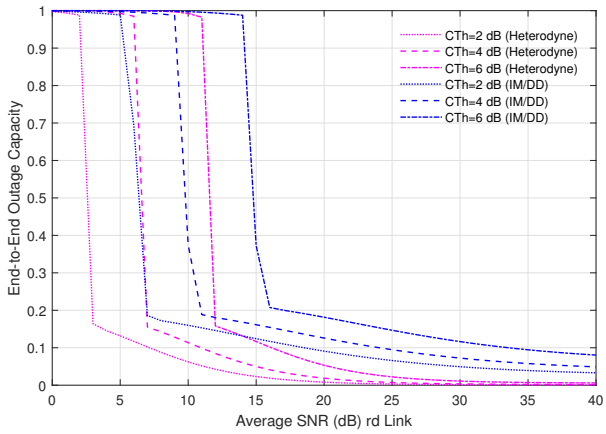

Fig. 7 Effects of capacity threshold on the end-to-end outage rate of Optical/Optical model for both Heterodyne detection and IM/DD technique under weak turbulence.

$m_i = 5$), the ergodic capacity increases as the strength of turbulence decreases.

Fig. 7 illustrates another crucial measure which is used to assess the system performance, that is outage capacity. In the figure, variations of outage capacity are demonstrated in respect of outage threshold for Optical/Optical underwater communication system. It can be clearly accounted that as we lower the threshold value, the throughput coverage becomes better. At some point, it can be seen that throughput coverage for heterodyne detection technique with $C_{Th} = 4$ dB is comparable to IM/DD technique with $C_{Th} = 2$ dB which proves its superiority.

6 Conclusion

In this paper, a hybrid dual hop UAOSN underwater monitoring system has been investigated using DF relay mechanism. The closed form expressions of equivalent PDF, CDF and moments have been derived. The system performance metrics include outage probability along with its high SNR behaviour, average BER, ergodic capacity and outage capacity. The system analysis is conducted for various acoustic parameteric conditions as well as optical turbulence to exhibit their effect on the performance of the system. The proposed system is designed to provide better coverage under sea with higher communication speed which serves as the better alternative to the traditional underwater acoustic communication systems.

Data Availability

The data (results and graphs) related to the findings of this study can be made available from the corresponding author upon reasonable request.

Conflict of Interest

There are no conflicts of interest to report.

References

1. Heidemann,J., Ye, W., Wills, J., Syed, A., Li, Y.: Research challenges and applications for underwater sensor networking. IEEE Wireless Communications and Networking Conference, 228-235 (2006)
2. Che, X., Wells, I., Dickers, G., Kear, P., Gong, X.: Reevaluation of RF electromagnetic communication in underwater sensor networks. IEEE Communications Mag. 48, 143-151 (2010). doi: 10.1109/MCOM.2010.5673085.
3. Akyildiz, I.F., Wang, P., Sun, Z.:Realizing underwater communication through magnetic induction.IEEE Communications Mag. 53, 42–48 (2015)
4. Stojanovic,M., Preisig, J.:Underwater acoustic communication channels: Propagation models and statistical characterization.IEEE Communications Mag. 47, 84–89 (2009)
5. Zeng, Z., Zhang, H., Dong, Y., Cheng, J. A Survey of Underwater Wireless Optical Communication. IEEE Communications Surveys Tutorials, (2016). doi:10.1109/COMST.2016.2618841
6. Xing, F., Yin, H., Ji, X., Leung, V.C.M.:An Adaptive and Energy-Efficient Algorithm for Surface Gateway Deployment in Underwater Optical/Acoustic Hybrid Sensor Networks. IEEE Communications Letters, 22, 1810-1813 (2018). doi: 10.1109/LCOMM.2018.2854279
7. Han, S., Noh, Y., Liang, R., Chen, R.S., Cheng, Y.J., Gerla, M.:Evaluation of underwater optical-acoustic hybrid network. China Communications, 11, 49–59 (2014)

8. Zhang, D., N'Doye, I., Ballal, T., Al-Naffouri, T.Y., Alouini, M.S., Laleg-Kirati, T.M.:Localization and Tracking Control Using Hybrid Acoustic–Optical Communication for Autonomous Underwater Vehicles. IEEE Internet of Things Journal, 7, 10048-10060 (2020). doi: 10.1109/JIOT.2020.2995799
9. Shen, Z., Yin, H., Jing, L., Liang Y., Wang, J.:A Cooperative Routing Protocol Based on Q-Learning for Underwater Optical-Acoustic Hybrid Wireless Sensor Networks. IEEE Sensors Journal, 22, 1041-1050 (2022). doi: 10.1109/JSEN.2021.3128594
10. Celik, A., Saeed, N., Shihada, B., Al-Naffouri, T.Y. Alouini, M.S.:Opportunistic Routing for Opto-Acoustic Internet of Underwater Things. IEEE Internet of Things Journal, 9, 2165-2179, (2022). doi: 10.1109/JIOT.2021.3090301
11. Hasna, M.O., Alouini M.S.:A performance study of dual-hop transmissions with fixed gain relays. IEEE Trans. Wireless Commun., 3, 1963-1968 (2004)
12. Zhang, W., Stojanovic, M., Mitra, U.:Analysis of a Linear Multihop Underwater Acoustic Network. IEEE Journal of Oceanic Engineering, 35, 961-970 (2010)
13. Sim˜ao, D.H., Chang, B.S., Brante, G., Pellenz, M.E., Souza, R.D.:Energy Efficiency of Multi-Hop Underwater Acoustic Networks Using Fountain Codes. IEEE Access, 8, 23110-23119 (2020)
14. Saeed, N., Celik, A., Alouini, M.S., Al-Naffouri, T.Y.:Performance Analysis of Connectivity and Localization in Multi-Hop Underwater Optical Wireless Sensor Networks. IEEE Transactions on Mobile Computing, 18, 2604-2615 (2019). doi: 10.1109/TMC.2018.2878672.
15. Celik, A., Saeed, N., Al-Naffouri, T.Y., Alouini, M.S.:Modeling and performance analysis of multihop underwater optical wireless sensor networks. 2018 IEEE Wireless Communications and Networking Conference (WCNC), 1–6 (2018)
16. Miridakis, N.I., Matthaiou, M., Karagiannidis, G.K.: Multiuser relaying over mixed RF/FSO links. IEEE Trans. Commun., 62, 1634–1645 (2014)
17. Anees, S., Bhatnagar, M.R.:Performance evaluation of decode-and-forward dual-hop asymmetric radio frequency-free space optical communication system. IET Optoelectron., 9, 232-240 (2015)
18. Gupta, A., Sharma, N., Garg, P., Jayakody, D.N.K., Aleksandrovich, C.Y., Li, J.: Asymmetric Satellite-Underwater Visible Light Communication System for Oceanic Monitoring. IEEE Access, 7, 133342-133350 (2019). doi:10.1109/ACCESS.2019.2936422
19. Elamassie, M., Miramirkhani, F., Uysal, M.: Performance Characterization of Underwater Visible Light Communication. IEEE Transactions on Communications, 67, 543-552 (2019). doi: 10.1109/TCOMM.2018.2867498
20. Chen, W., Yu, H., Guan, Q., Ji, F., Chen, F.: Reliable and Opportunistic Transmissions for Underwater Acoustic Networks. IEEE Network, 32, 94-99 (2018). doi: 10.1109/MNET.2018.1700280
21. Radosevic, A., Proakis, J.G., Stojanovic, M.: Statistical characterization and capacity of shallow water acoustic channels," OCEANS 2009-EUROPE, 2009, pp. 1-8, doi: 10.1109/OCEANSE.2009.5278349.
22. Nouri, H., Uysal, M., Panayirci, E.: Information theoretical performance analysis and optimisation of cooperative underwater acoustic communication systems. IET Communications, 10, 812-823 (2016)
23. Jalil, A.M., Ghrayeb, A.:Distributed Channel Coding for Underwater Acoustic Cooperative Networks. IEEE Transactions on Communications, 62, 848-856 (2014). doi: 10.1109/TCOMM.2014.012314.130425
24. Wang, C., Wang, Z., Sun, W., Fuhrmann, D.R.: Reinforcement Learning-Based Adaptive Transmission in Time-Varying Underwater Acoustic Channels. IEEE Access, 6, 2541-2558 (2018). doi: 10.1109/ACCESS.2017.2784239
25. Badarneh, O.S.: The α-$\mathcal{F}$ Composite Fading Distribution: Statistical Characterization and Applications. IEEE Transactions on Vehicular Technology, 69, 8097-8106 (2020). doi: 10.1109/TVT.2020.2995665
26. Sun, Q., Zhang, Z., Zhang, Y., López-Benítez, M., Zhang, J.:Performance Analysis of Dual-Hop Wireless Systems Over Mixed FSO/RF Fading Channel. IEEE Access, 9, 85529-85542 (2021). doi: 10.1109/ACCESS.2021.3085821
27. Gercekcioglu, H.: Bit error rate of focused Gaussian beams in weak oceanic turbulence. Journal of the Optical Society of America A, 31, 1963–1968 (2014)
28. Yi, X., Li, Z., Liu, Z.: Underwater optical communication performance for laser beam propagation through weak oceanic turbulence. Applied Optics, 54, 1273–1278 (2015)
29. Jamali, M.V., Khorramshahi, P.A.T., Chizari, A., Shahsavari, S., AbdollahRamezani, S., Fazelian, M., Bahrani, S., Salehi, J.A.: Statistical distribution of intensity fluctuations for underwater wireless optical channels in the presence of air bubbles. Iran Workshop on Communication and Information Theory, Tehran, Iran, May 2016, pp. 1–6.
30. Oubei, H.M., Zedini, E., ElAfandy, R.T., Kammoun, A., Ng, T.K., Hamdi, M., Alouini, M.S., Ooi, B.S.: Efficient Weibull channel model for salinity induced turbulent underwater wireless optical communications. 22nd OptoElectronics and Communications Conference, (2017)
31. Oubei, H.M., Zedini, E., ElAfandy, R.T., Kammoun, A., Abdallah, M., Ng, T.K., Hamdi, M., Alouini, M.S., Ooi, B.S.: Simple statistical channel model for weak temperature-induced turbulence in underwater wireless optical communication systems. Optics Letters, 42, 2455–2458 (2017)
32. Zedini, E., Oubei, H.M., Kammoun, A., Hamdi, M., Ooi, B.S., Alouini, M.S.: A new simple model for underwater wireless optical channels in the presence of air bubbles. IEEE Global Communications Conference (GLOBECOM'17), 1–6 (2017)
33. Zedini, E., Oubei, H.M., Kammoun, A., M. , Hamdi B.S., Alouini, M.S.: Unified Statistical Channel Model for Turbulence-Induced Fading in Underwater Wireless Optical Communication Systems. IEEE Transactions on Communications, 67, 2893-2907 (2019). doi: 10.1109/TCOMM.2019.2891542
34. Bhatnagar, R., Garg, P.:Hybrid Underwater Wireless System for Shallow Sea Monitoring: An Outage Analysis. 2022 IEEE International Conference on Electronics, Computing and Communication Technologies (CONECCT), 1-5 (2022). doi: 10.1109/CONECCT55679.2022.9865697
35. Prudnikov, A.P., Brychkov, J.A., Marichev, O.I.: Integrals and Series: More Special Functions. New York, USA (1990)
36. Olver, F.W., Lozier, D.W., Boisvert, R.F., Clark, C.W.: NIST handbook of mathematical functions hardback and CD-ROM, Cambridge university press (2010)
37. Gradshteyn, I.S., Ryzhik, I.M.: Table of Integrals, Series, and Products, California (2007)
38. Kilbas, A.A.:H-Transforms: Theory and Applications. Boca Raton, USA (2004)
39. Ashrafzadeh, B., Soleimani-Nasab, E., Kamandar, M., Uysal, M.:A framework on the performance analysis

of dual-hop mixed FSO-RF cooperative systems. IEEE Trans. Wireless Commun., 67, 4939–4954 (2019)
40. Zedini, E., Zedini, Soury, H., Alouini, M.S.:On the performance analysis of dual-hop mixed FSO/RF systems. IEEE Trans. Wireless Commun., 15, 3679–3689 (2016)
41. Wolfram Research,Inc.http://functions.wolfram.com.
42. Zedini, E., Soury, H., Alouini, M.S.:Dual-Hop FSO transmission systems over Gamma-Gamma turbulence with pointing errors. IEEE Transactions on Wireless Communications, 16, 784–796 (2017)
43. Badarneh, O.S., Costa, D.B., Benjillali, M., Alouini, M.:Selection Combining Over Double α-μ Fading Channels. IEEE Transactions on Vehicular Technology, 69, 3444-3448 (2020). doi: 10.1109/TVT.2020.2969224
44. Balti, E., Guizani, M.:Mixed RF/FSO Cooperative Relaying Systems With Co-Channel Interference. IEEE Transactions on Communications, 66, 4014-4027 (2018). doi:10.1109/TCOMM.2018.2818697.